Prediction of drug loading in the gelatin matrix using computational methods

Rania M. Hathout [1]*, AbdelKader A. Metwally [1,2], Timothy J. Woodman [3] and John G. Hardy [4,5]*

[1] Department of Pharmaceutics and Industrial Pharmacy, Faculty of Pharmacy, Ain Shams University, Cairo, 11566, Egypt.; rania.hathout@pharma.asu.edu.eg (R.M.H.); AbdelKader74@yahoo.com (A.A.M).

[2] Department of Pharmaceutics, Faculty of Pharmacy, Health Sciences Center, Kuwait University, Kuwait; AbdelKader74@yahoo.com (A.A.M).

[3] Department of Pharmacy and Pharmacology, University of Bath, Bath, BA2 7AY, UK.; T.Woodman@bath.ac.uk (T.J.W.).

[4] Department of Chemistry, Lancaster University, Lancaster, Lancashire, LA1 4YB, UK.; j.g.hardy@lancaster.ac.uk (J.G.H.).

[5] Materials Science Institute, Lancaster University, Lancaster, Lancashire, LA1 4YB, UK.

* Correspondence: rania.hathout@pharma.asu.edu.eg (R.M.H.); j.g.hardy@lancaster.ac.uk (J.G.H.).

Abstract

The delivery of drugs is a topic of intense research activity in both academia and industry with potential for positive economic, health, and societal impacts. The selection of the appropriate formulation (carrier and drug) with optimal delivery is a challenge investigated by researchers in academia and industry, in which millions of dollars are invested annually. Experiments involving different carriers and determination of their capacity for drug loading is very time consuming, and therefore expensive; consequently, approaches that employ computational/theoretical chemistry to speed have the potential to make hugely beneficial economic, environmental and health impacts through savings in costs associated with chemicals (and their safe disposal) and time. Here we report the use of computational tools (data mining of available literature, principal component analysis, hierarchical clustering analysis, partial least squares regression, autocovariance calculations, molecular dynamic simulations and molecular docking) to successfully predict drug loading into model drug delivery systems (gelatin nanospheres). We believe that this methodology has the potential to lead to significant change in drug formulation studies across the world.

Keywords: drug delivery; computational pharmaceutics; machine learning; molecular dynamics simulations; docking; formulations; nanoparticles; gelatin.

1. Introduction

The global market for drug-delivery systems is a multibillion-dollar industry, demand for which is growing in both developed and emerging economies (in part, driven by aging societies and rapid urbanization) [1-9]. Drug-delivery systems deliver drugs at rates controlled by specific features of the systems, particularly their chemical composition (e.g., inorganic/organic components, molecular weights of their constituents, crosslinking density of polymers, etc.) [10-12].

The selection of the appropriate system (carrier and drug) to obtain optimal delivery is a challenge investigated by researchers in academia and industry, in which millions of dollars are invested annually [13]. Experiments involving different carriers and determination of their capacity for drug loading is very time consuming, and therefore expensive. Consequently, approaches that exploit multivariate statistical methods, molecular simulations, docking methods, and mining the data in the literature [14-19], have the potential to make hugely beneficial economic, environmental and health impacts through savings in costs associated with chemicals (and their safe disposal) and time.

Computational/theoretical chemists/biochemists, biomedical/chemical engineers and pharmacists have developed a variety of methodologies that can be applied to understand drug formulations. Principal component analysis (PCA) and hierarchical clustering analysis (HCA) are considered exploratory data analysis and unsupervised machine learning methods, where these techniques extract patterns from the independent factors (x-variables) only and irrelevant to the y-outcomes. Partial least squares (PLS) is a supervised pattern recognition method correlating the inputs with outputs and subsequently leads to the generation of a model [20]. This data mining approach (through a retrospective analysis) combined with computer-aided analysis and simulation extracts knowledge from complex variables and responses obtained from historical records. The significant advantage of this

approach is the possibility of uncovering interactions and linear relationships that might not be easily detectable with conventional experimental designs [21]. Although not yet fully explored in drug formulation/delivery, multivariate statistical methods such as PCA and agglomerative HCA were previously used to develop drug delivery formulations. For example, PCA was utilized to generate a quantitative composition-permeability relationship for microemulsion formulations used to deliver testosterone transdermally, with a linear relationship between the lower-dimensionality data generated from the main principal component and the permeability coefficients of the different formulations [22]. PCA and HCA were used to extract stable SMEDDS (Self Microemulsifying Drug Delivery Systems) and SNEDDS (Self Nanoemulsifying Drug Delivery Systems) formulations of Lovastatin and Glibenclamide, respectively [23,24]; and PCA and PLS analysis were used to assess the qualitative and quantitative effects of different variables such as lipid/surfactant type and their concentrations on parameters related to storage stability [25]. Furthermore, PLS was successfully employed to predict the sizes and polydispersity index (PDI) for lipid nanocapsules based on the quantitative mixture composition [26].

Here we extend these exciting studies by combining PCA, HCA and PLS with molecular dynamics and docking analysis [27] to give valuable insight into drug loading in a polymer matrix. As a model polymer matrix we use protein-based nanoparticulate drug delivery systems (i.e. nanospheres composed of collagen-derived gelatin). Gelatin is an abundant and inexpensive protein [28], which is amphiphilic in nature due to its amino acid contents (ca. 12% anionic glutamic and aspartic acid; ca. 13% cationic lysine and arginine amino acids, and ca. 11% hydrophobic leucine, isoleucine, methionine and valine) [29], and gelatin-based matrices can in principle be used to deliver both small molecules and macromolecules [30-36]. In this study we focus on a selection of low molecular weight drugs used in the clinic as depicted in **Figure 1**.

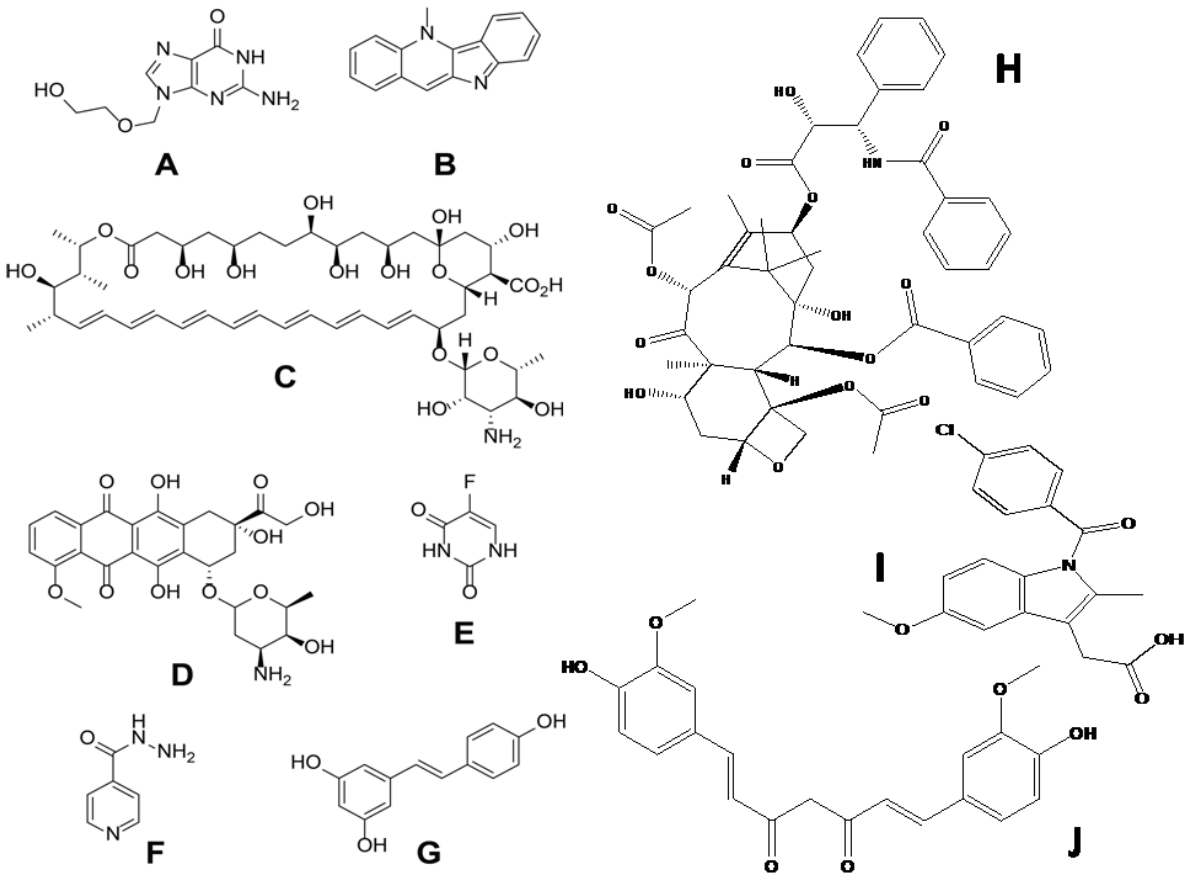

Figure 1. The chemical structures of the substances studied herein: A) Acyclovir, B) Cryptolepine, C) Amphotericin B, D) Doxorubicin, E) 5-Fluorouracil (5FU), F) Isoniazid, G) Resveratrol, H) Paclitaxel, I) Indomethacin and J) Curcumin.

2. Materials and Methods

2.1. Data set

The data set contained 4 input variables (descriptors) and one output response (mass of drug loaded per 100 mg gelatin nanospheres determined experimentally) for different drugs. Data mining was performed through different databases such as: Pubmed and Web of Science® to obtain the output response for ten drugs: Acyclovir [37], Amphotericin B [38], Cryptolepine [39], Doxorubicin [40], 5 Fluorouracil (5FU) [41], Isoniazid [42], Resveratrol [43], curcumin [44], paclitaxel [45] and indomethacin [46].

118

119 *2.2. Calculation of molecular descriptors*

120 The drugs were analyzed using Bioclipse® version 2.6 (Bioclipse project, Uppsala
121 University, Sweden) [39]. The four descriptors chosen were constitutional (molecular
122 weight), electronic (number of hydrogen bond donors and number of hydrogen bond
123 acceptors) and physico-chemical (xLog P).

124

125 *2.3. Hierarchical clustering analysis (HCA).*

126 The molecular descriptors generated using Bioclipse® version 2.6 were subjected to
127 Hierarchical Clustering Analysis using JMP® 7.0 (SAS, Cary, NC, USA). Ward's minimum
128 variance method was adopted to join the clusters and generate a dendrogram. Ward's method
129 is considered an agglomerative hierarchical technique where the merging in the dendrogram
130 starts at the final clusters (leaves) and merging occurs stepwise until it reaches the trunk.
131 Ward's minimum variance criterion minimizes the total within-cluster variance. At each step,
132 the pair of clusters possessing minimum between-cluster distance is merged (i.e. the pair of
133 clusters that leads to the minimum increase in the total within-cluster variance after merging
134 is selected) [47] .

135

136 *2.4. Principal component analysis (PCA).*

137 PCA was used to extract patterns using an exploratory data analysis method that deals
138 with the variances in sample observations. PCA was performed using JMP® 7.0. Four
139 principal components were calculated by taking a linear combination of an eigenvector of the
140 correlation matrix built up from standardized original variables. The dimensionality of the
141 data was reduced by extracting two main principal components possessing the two highest
142 Eigen values and plotting the data with respect to these two new orthogonal axes.

143

2.5. Partial least squares analysis (PLS) for model generation and validation of the model.

PLS was used to study correlations between the molecular descriptors and the output response. PLS was performed using JMP® 7.0 using 4 latent vectors. The PLS generated model was validated by checking the differences between the mean actual and predicted response values using t-test statistical analysis at $P < 0.05$ using GraphPad Prism® v.5.0 (GraphPad software Inc., San Diego, CA, USA) and by performing a k-fold (5-folds) cross-validation (leave-two-out) to check the predictability of the model and its ability to navigate the experimental space. The value of Q^2 (Predicted R-squared) was calculated as follows:

$$Q^2 = \frac{PRESS}{ISS}$$

Where PRESS represents the predicted residual error sum of squares while ISS stands for the total initial sum of squares. Moreover, a predicted versus actual correlation was obtained.

2.6. Molecular dynamics simulations (MDS) of the gelatin matrix.

Molecular dynamics simulations (MDS) were carried-out using the GROMACS [48] v. 4.6.5 freeware (http://www.gromacs.org/). To prepare the gelatin system, 48 peptide molecules were constructed, with 18 amino acids in each molecule. The primary sequence of the peptides was AGPRGQ(Hyp)GPAGPDGQ(Hyp)GP. Six hypothetical probe molecules (with calculated molecular weight of 767.13) were added at random positions to the system. The force field parameters were obtained from CgenFF [49] (https://cgenff.paramchem.org/). The system was energy minimized by the steepest descent method. Molecular dynamics was subsequently carried-out, with a time step of 2 fs, full periodic boundary conditions, and a cut-off distance of 1.2 nm for Van der Waal's and electrostatic interactions [50]. PME was chosen to handle long-range electrostatic interactions. All bonds were constrained by the LINCS algorithm. The MDS were carried-out for 3 ns, at 373K and 1 bar using a v-rescale thermostat and a Berendsen barostat respectively [51].

2.7. Drug docking in simulated gelatin nanospheres.

The chemical structures of the studied drugs were drawn using ChemDraw® Ultra version 10 (Cambridgesoft, Waltham, MA, USA). The corresponding '.mol2' files needed for docking experiments were obtained using Chem3D® Ultra version 10 (Cambridgesoft, Waltham, MA, USA) after energy minimization using the MM2 force field of the same program. Docking analysis was generated by Argus Lab version 4.0.1. (Mark Thompson and Planaria Software LLC, Seattle, WA, USA). The hypothetical probe molecules were utilized to construct corresponding binding sites on the carrier (gelatin-probe), the AScore was utilized for calculating the scoring function. The size of the display box in the x, y and z dimensions were 15 x 15 x15 Å as these dimensions were suitable to the size of the docked molecules and ensured a central position for them inside the gelatin matrix. Additionally, the genetic algorithm was used as the docking engine with 150 maximum poses. The type of calculation and ligand (as chosen using the software options) were Dock and Flexible, respectively; and the binding energies (ΔG, kcal/mole) reflecting the docking efficiencies were calculated.

3. Results

Table 1 reports the molecular descriptors (number of hydrogen bond donors, number of hydrogen bond acceptors, xLogP and molecular weight) for the investigated drugs. The dendrogram classifying these drugs according to HCA using Ward's minimum variance method (an agglomerative type of analysis) is displayed in **Figure 2**. Isoniazid and 5FU were clustered together according to their 4 descriptors, Resveratrol and Cryptolepine clustered together, whereas Doxorubicin, Acyclovir and Amphotericin B constituted separate clusters. Importantly, the loading pattern followed this classification (see Table 1) where 5FU and Isoniazid scored the highest loading masses followed by Acyclovir which is closest to the

196 aforementioned drugs in the dendrogram. Cryptolepine and Reseveratrol were very close,
197 with Doxorubicin near to them. Amphotericin B had the lowest mass loaded into the
198 nanospheres which was clear from its separate branch (furthest distance) in the dendrogram.

199 **Table 1.** The descriptors of the drugs, amounts of loaded drug, and the obtained
200 binding energies from docking of the drugs on a simulated gelatin matrix.

Drug	xLogP	No. H-bond donors	No. H-bond acceptors	Molecular Weight (g/mol)	Actual Amount of Drug Loaded (mg/100mg gelatin)	Lamarckian Genetic Algorithm ΔG (kcal/mole)
Acyclovir	-1.650	3	8	225.21	8.74	-3.94
Amphotericin B	2.068	12	18	923.49	1.16	144.4
Cryptolepine	2.180	0	2	233.30	2.00	-3.81
Doxorubicin	-1.900	6	9	543.52	2.10	58.29
5-Fluorouracil	-0.760	2	4	130.00	25.07	-4.19
Isoniazid	-0.683	3	4	137.14	22.00	-4.16
Resveratrol	2.050	3	3	228.24	1.96	-3.74
Curcumin	1.95	2	6	368.13	3.50	-2.59
Paclitaxel	6.15	4	14	853.33	0.52	173.5
Indomethacin	3.78	1	4	338.14	1.91	-1.99

201

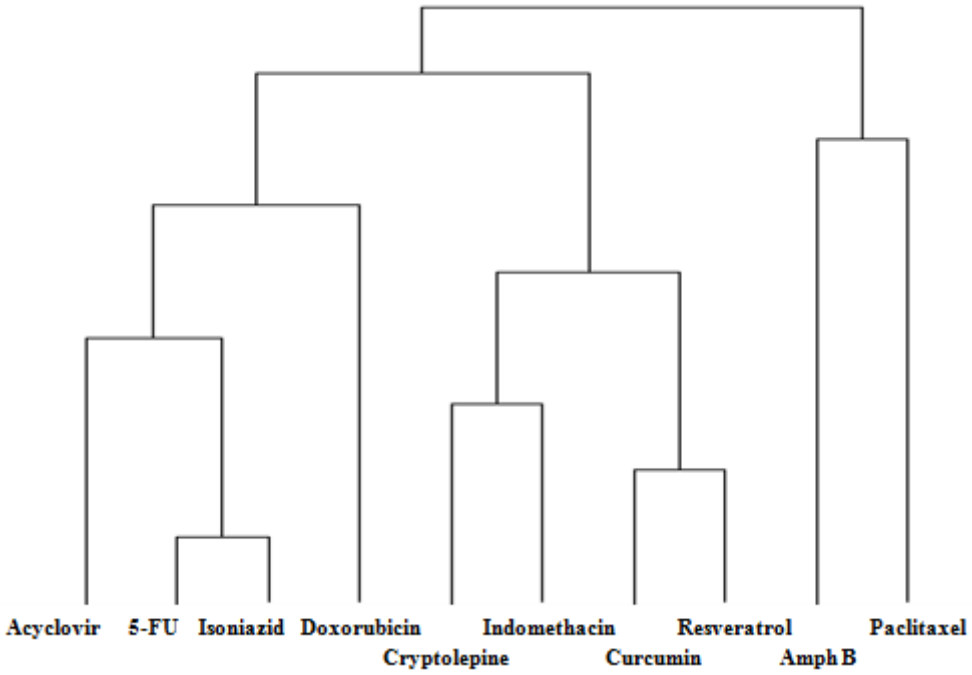

Figure 2. Hierarchical Clustering Analysis (HCA) of the investigated drugs with respect to 4 constitutional, electronic and physico-chemical descriptors: number of hydrogen bond donors, number of hydrogen bond acceptors, xLogP and molecular weight.

A score plot of the drugs with respect to their descriptors after projecting the data into two main principal components is displayed in **Figure 3**, where principal component 1 and principal component 2 reflect 69.72% and 26.95 % of the data variation, respectively (corresponding to 96.68 % of total variance, **Figure 3**, top right panel) and 5FU and Isoniazid are clustered together with Acyclovir having the nearest score, and Amphotericin B the furthest score. Figure 4 depicts the loading plots of the two main principal components. It is obvious that principal component 1 is mainly composed of the descriptors; the molecular weight, the number of the H-bond donors and the number of the number of H-bond acceptors while principal component 2 mainly depends on the remaining descriptor; xLogP. These results confirm the presentation of the 4 investigated variables in the two generated principal components.

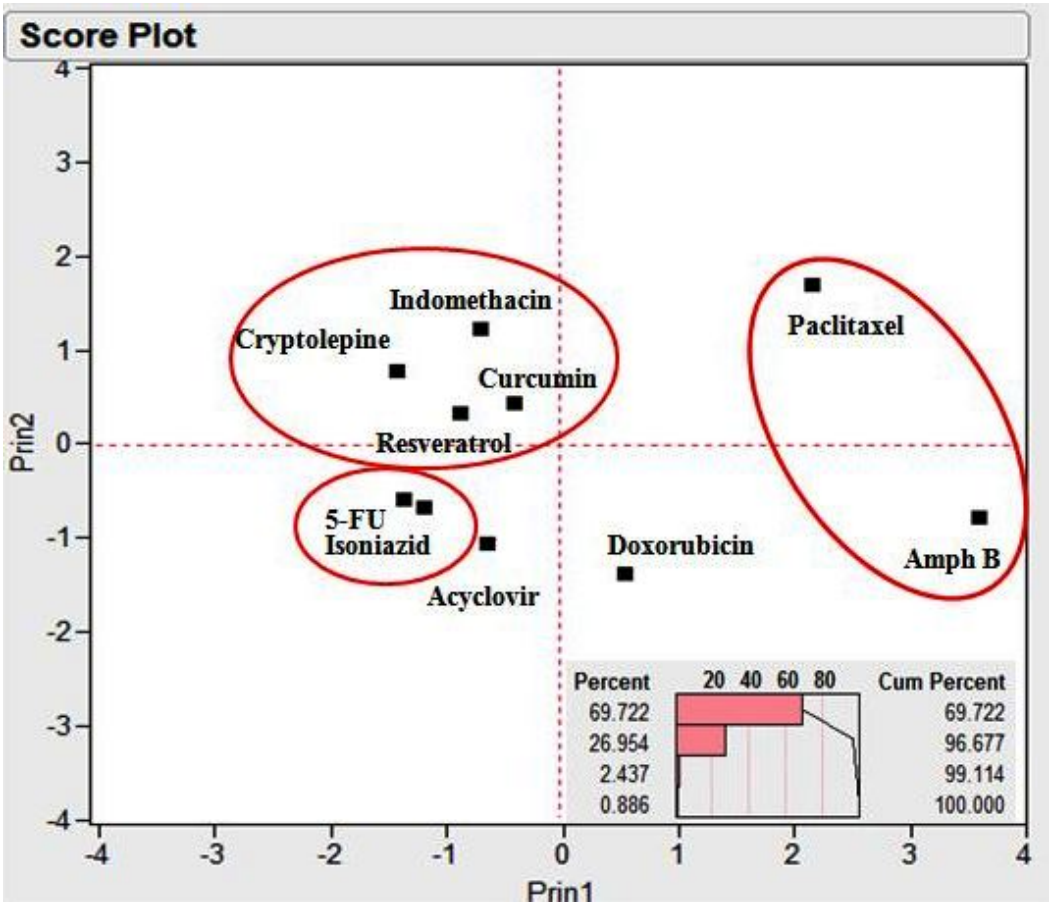

Figure 3. Principal Component Analysis (PCA) score plot of the investigated drugs with respect to 4 constitutional, electronic and physico-chemical descriptors: number of hydrogen bond donors, number of hydrogen bond acceptors, xLogP and molecular weight, displaying only two main combined components. The upper panel depicts the scree plot revealing the percentage variation of each extracted component (combined from the four descriptors).

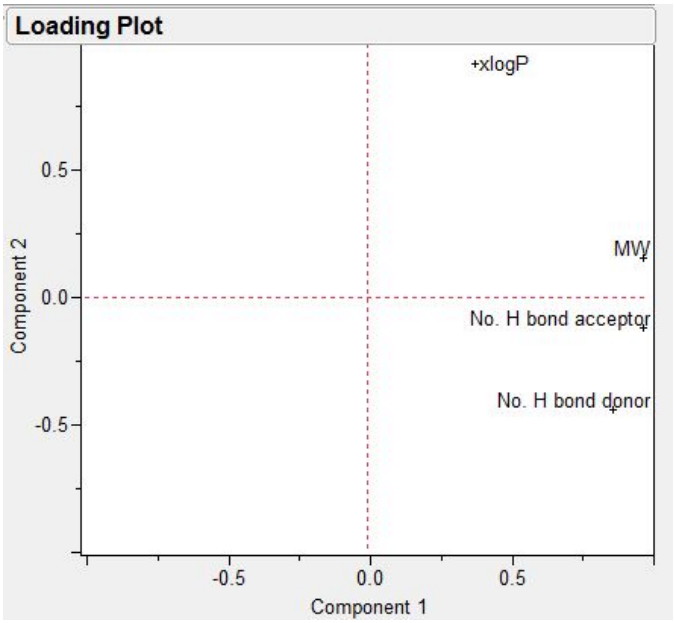

227

228 **Figure 4.** Principal Component Analysis (PCA) loading plot of the two main principal
229 components.

230

231 The relationship between the obtained combined x-scores (combining the contribution
232 from the 4 x-variables *viz.* descriptors) and y-scores is displayed in **Figure 5**, and the scree
233 plot (**Figure 5**, bottom right) depicts the contribution of each individual latent factor to the
234 combined x-scores with the first two factors accounting for 96.64% of the obtained scores.

235

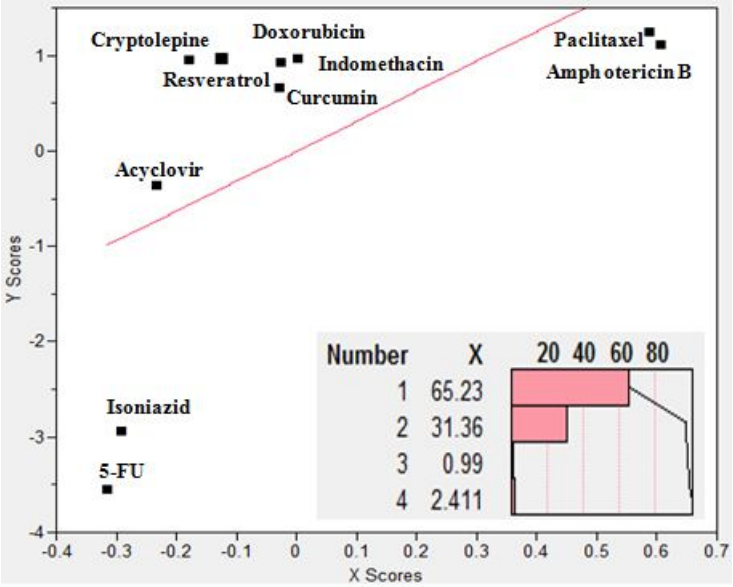

236

Figure 5. Partial Least Squares Regression Analysis (PLS) of the investigated drugs with 4 constitutional, electronic and physico-chemical descriptors: number of hydrogen bond donors, number of hydrogen bond acceptors, xLogP and molecular weight as the x-factors and the mass of loaded drug per 100 mg gelatin nanoparticles as the y-factor. The lower panel depicts the contribution of each latent x-factor (combined factor) to the x-scores representing the combined x-dimension.

It is noteworthy that the generated x- and y- scores represent the distances of the points in space of all the dimensions to the main vector summarizing the final dimension (in the current case there is a principal component or vector for the x-dimension comprising all the descriptors, and another for the y-dimension representing the loaded mass). Therefore, the aforementioned scores can be negative numbers. Consequently, a generated model was developed where:

$$\begin{aligned} Y\ (\text{mass of drug loaded per 100 mg of gelatin nanoparticles}) = 13.175 + 0.115 \times \\ \text{xLogP} + 0.001 \times \text{number of hydrogen bond donors} + 2.346 \times \text{number of} \\ \text{hydrogen acceptors} - 0.059 \times \text{molecular weight.} \end{aligned} \quad (1)$$

The values and the signs of the coefficients of the x-factors in the equation were indicative of the importance of increasing the number H- bond acceptors in the drugs chemical structure in the presence of a balanced xlogP and low molecular weight to increase the loading of the drug. The model was validated by performing a t-test statistical analysis between the actual experimental results for drug loading and the predicted drug loading using the model where no significant difference was obtained between the means at $P < 0.05$. The calculated Q^2 or the predicted r-squared after 5-folds cross-validation scored a value of 0.721 (a highly acceptable value) [52]. Figure 6 further demonstrates the predicted versus actual relationship where it is observed that most of the points are scattered around the 45° line. Proximity of the points to this line usually indicates the favorable similarity of the results.

Accordingly, the developed model can be exploited in predicting the loaded mass of any new physically loaded or entrapped investigated drug molecule in a gelatin matrix after projecting its structure to the aforementioned four descriptors (**Table 1**).

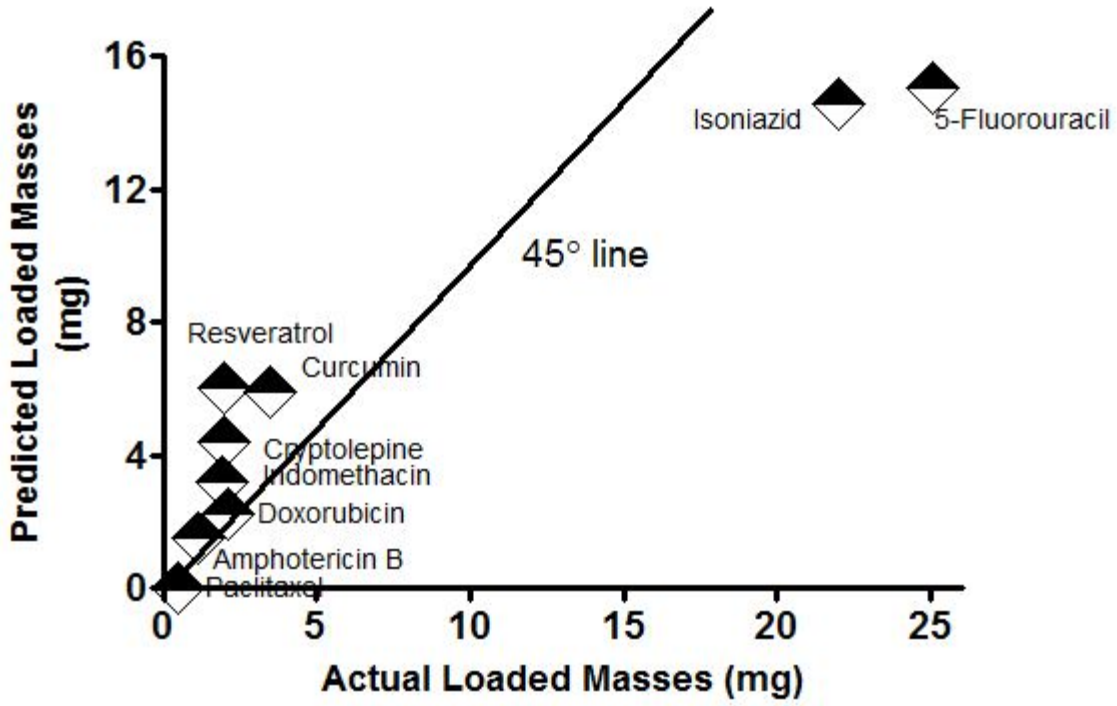

Figure 6. Predicted versus actual drug loading in gelatin nanospheres.

4. Discussion

In the HCA utilized and studied method (Ward's method), the distance between two clusters is the ANOVA sum of squares between the two clusters added up over all the variables. At each generation, the within-cluster sum of squares is minimized over all partitions obtainable by merging two clusters from the previous generation. The sums of squares are usually easily interpreted when they are divided by the total sum of squares to give the proportions of variance (squared semi-partial correlations). Ward's method works under the assumptions of spherical covariance matrices and the condition of equal sampling probabilities. Distances between clusters in Ward's method are calculated according to the

squared Euclidean distance. It is considered very useful in joining clusters with a small number of observations and it is very accurate though sensitive to outliers [53].

PCA was used to confirm the hierarchical clustering analysis results. This type of multivariate analysis deals with the x-factors (descriptors) to reduce their dimensionality by projecting the data into new orthogonal axes that display the directions (vectors) of the highest variation. These results confirmed the HCA results and correlate the x-factors (drug descriptors) with the y-outputs (mass of drug loaded per 100 mg of gelatin) where clustered points (Especially in the same quadrants) represents high similarity between them regarding their projected descriptors [54].

Accordingly, a supervised learning tool (PLS) was used to generate an accurate and sensitive model that would correlate the x-factors with the y-outputs quantitatively. The techniques implemented in the PLS platform work by extracting successive linear combinations of the predictors, called factors (also called components or latent vectors), which optimally address the combined goals of explaining both response and predictor variation. In particular, the method of PLS balances the two objectives and maximizes their correlation [55].

The obtained results can be explained by the fact that gelatin is a protein carrier with a relatively balanced hydrophilic/hydrophobic character displaying several hydrogen bond donor and acceptor groups with a repetitive sequence of amino acids -Ala-Gly-Pro-Arg-Gly-Glu-4Hyp-Gly-Pro- along its backbone [56]. This structure can be transformed to some numerical values that are generated of each amino acid. Among which are the highly condensed variables “z-scale descriptors” [57] that are derived from a PCA analysis of several experimental and physicochemical properties of the 20 natural amino acids; z1, z2, and z3 and which represent the amino acids hydrophobicity, steric properties, and polarity, respectively. Additionally, they are useful in QSAR analysis of peptides where they have proven effective in predicting different physiological activities [58-60]. Herein, we

used an extended scale (including 67 more artificial and derivatized amino acids) [61] due to the presence of 4-hydroxyproline in the gelatin structure.

In this study, we expand the use of the first descriptor (z1) to predict the drug loading properties of nanoparticles. The first scale (z1) was chosen as it represents a lipophilicity scale that encompasses several variables (amino acid descriptors) such as: the thin layer chromatography (TLC) variables, log P, nonpolar surface area (Snp) and polar surface area (Spol) in combination with the number of proton accepting electrons in the side chain (HACCR) [62]. In this scale, a large negative value of z1 corresponds to a lipophilic amino acid, while a large positive z1 value corresponds to a polar, hydrophilic amino acid. Therefore, the gelatin typical structure amino acids (-Ala-Gly-Pro-Arg-Gly-Glu-4Hyp-Gly-Pro-) can be represented by their z1 values as follows: (0.24), (2.05), (-1.66), (3.52), (2.05), (3.11), (-0.24), (2.05) and (-1.66). Furthermore, an overall topological description of the repetitive sequence was accounted for by encoding the z1 descriptors of each amino acid into one auto covariance variable [49] that was first introduced by Wold et al. [63]. The auto covariance value (AC) was calculated as follows: $AC_{z.lag} = \sum_{i=1}^{N-lag} \frac{V_{z.i} \times V_{z,i+lag}}{N-lag}$ (2)

$$AC_{z.lag} = \sum_{i=1}^{N-lag} \frac{V_{z.i} * V_{z,i+lag}}{N-lag} \quad (2)$$

where AC represents autocovariances of the same property (z-scale); i = 1, 2, 3,...; N is the number of amino acids; lag = 1, 2, 3, ... L (where L is the maximum lag which is the longest sequence used and V is the scale value).

Therefore, the AC value for the gelatin typical structure sequence was calculated with lag 1 scoring a value approaching zero (0.028) indicating a balanced hydrophobicity/hydrophilicity structure. In light of the above, the high loading of 5FU and Isoniazid can be ascribed to their amphiphilic nature with LogP values approaching 0, and to

the presence of several hydrogen bond donors and acceptors groups relative to their low molecular weight that is favorable in both diffusion through and entrapment in a protein matrix like that of gelatin nanospheres. Since there was a recorded deviation between the actual and the predicted values regarding Isoniazid and 5FU (may be attributed to their small molecular weight that helps their non-stoichometric physical entrapment in the gelatin matrix, therefore, the results were further confirmed by molecular dynamics and docking experiments, where the drugs were docked on the gelatin matrix simulated structure. **Figure 7** shows the molecular simulation of the gelatin nanosphere matrix. Interestingly, the best binding energy values ΔG (- 4.19 and -4.16 kcal/mol) corresponded to the highest loaded drugs 5FU and Isoniazid, respectively, followed by Acyclovir (see **Figure 8**). In the same context, Amphotericin B scored a highly positive ΔG value which explains its low loading values. The confirmation of the docking results with their experimental counterparts can be attributed to the inclusive scoring function of the Arguslab® software. This scoring function is based on the XScore calculated according to the following equation [64]:

$$\Delta G_{bind} = \Delta G_{vdw} + \Delta G_{hydrophobic} + \Delta G_{H\text{-}bond} + \Delta G_{H\text{-}bond\ (chg)} + \Delta G_{deformation} + \Delta G_0 \quad (3)$$

where ΔG_{bind} is the total calculated binding energy, ΔG_{vdw} is the binding energy due to Van der Waal's forces, $\Delta G_{hydrophobic}$ is the binding energy due to hydrophobic forces, $\Delta G_{H\text{-}bond}$ is the binding energy due to H-bonding, $\Delta G_{H\text{-}bond\ (chg)}$ is the binding energy due to H-bonding due to charged molecules, $\Delta G_{deformation}$ is the energy due to rotational bonds and atoms involved in torsions (rotors) that were frozen due to binding, and finally, ΔG_0 represents the regression-obtained binding energy. As can be inferred, the equation terms encompass nearly all the possible interactions that can occur between the drug and its carrier that may lead to drug entrapment which explains the high correlation obtained between the real experimental values and the docking results.

An exponential model was generated correlating the actual experimental molar masses of the loaded drugs and their corresponding docking binding energies. This model was highly

348 fitting with an obtained r-squared value of 0.95. This relationship can highly estimate the
349 molar masses of physically loaded drugs through docking the investigated molecule on the
350 simulated gelatin matrix. The only limitation of the model was the number of the
351 experimental studies that are involved in it (10 studies) which we recommend to increase in
352 further similar studies.

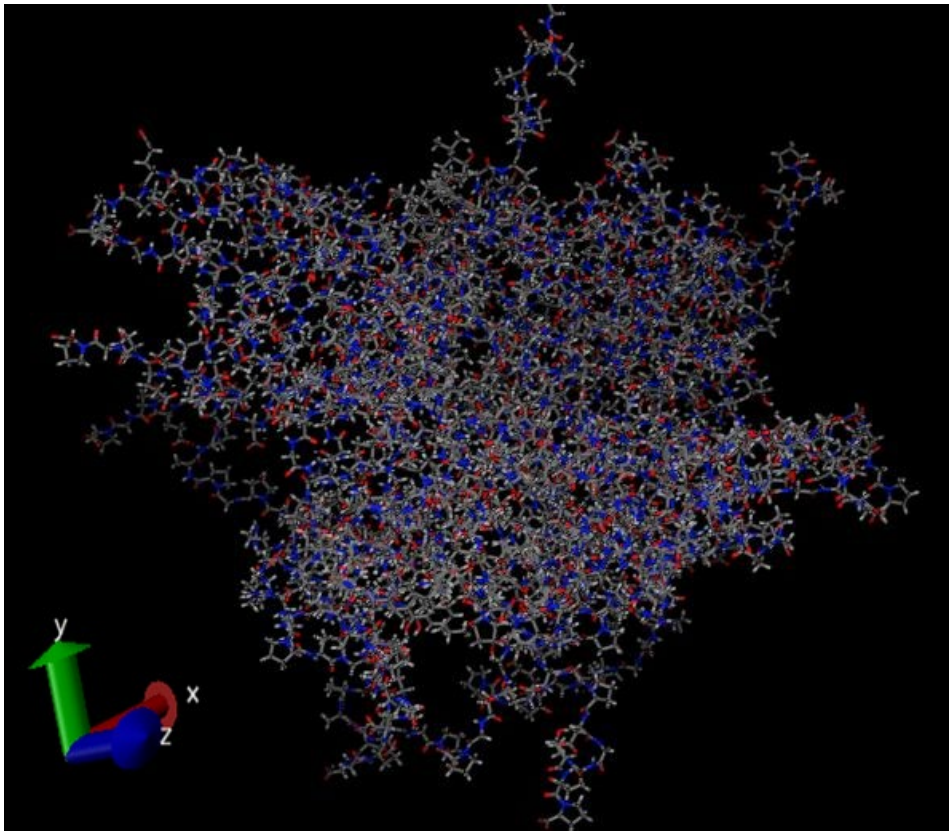

353

354

355 **Figure 7.** Molecular dynamics simulation of the gelatin nanosphere matrix.

356

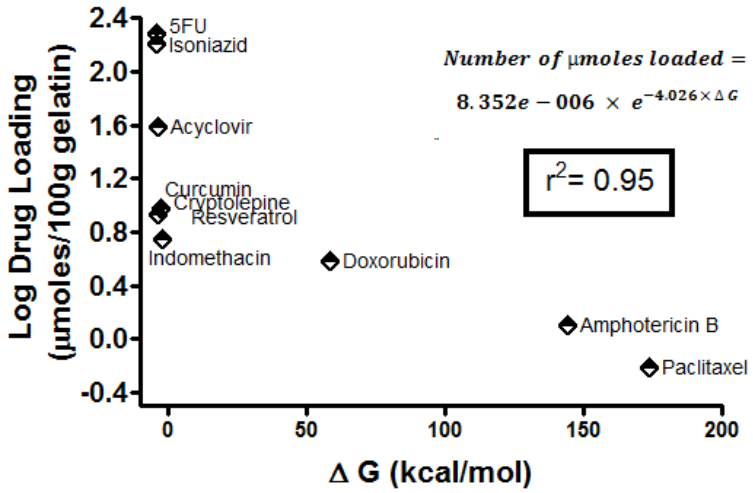

Figure 8. Drug loading versus the obtained binding energies plot of the investigated drugs after docking on a simulated gelatin matrix built up using molecular dynamics simulation displaying an exponential relationship.

5. Conclusions

The current study introduces new approaches of interpreting and predicting drugs loading on protein carriers, such as gelatin nanospheres. These approaches comprise multivariate statistical methods such as: hierarchical clustering analysis, principal component analysis, partial least squares regression, molecular dynamics and docking. Moreover, the utilization of the amino acids z-scales descriptors represents a new and important asset in interpreting drug loading in protein-based carriers. We believe that this methodology has the potential to lead to significant change in drug formulation studies across the world.

Funding: There are no funding sources to report.

Conflicts of Interest: The authors declare no conflict of interest .

References

1. **Bae, Y. H. Stimuli-Sensitive Drug Delivery. In *Controlled Drug Delivery: Challenge and Strategies*, Park, K., Ed.; American chemical Society: Washington, 1997; pp 147-160.**

2. **Hoffman, A. S. Intelligent Polymers. In *Controlled Drug Delivery: Challenge and Strategies*, Park, K., Ed.; American chemical Society: Washington, 1997; pp 485-497.**

3. **Kanjickal, D. G.; Lopina, S. T. Modeling of drug release from polymeric delivery systems--a review. *Crit Rev. Ther. Drug Carrier Syst.* 2004, *21* (5), 345-386.**

4. **Kumar, M.; Curtis, A.; Hoskins, C. Application of Nanoparticle Technologies in the Combat against Anti-Microbial Resistance. *Pharmaceutics* 2018, *10* (1).**

5. **Liechty, W. B.; Kryscio, D. R.; Slaughter, B. V.; Peppas, N. A. Polymers for drug delivery systems. *Annu. Rev. Chem. Biomol. Eng* 2010, *1*, 149-173.**

6. **Manzur, A.; Oluwasanmi, A.; Moss, D.; Curtis, A.; Hoskins, C. Nanotechnologies in Pancreatic Cancer Therapy. *Pharmaceutics* 2017, *9* (4).**

7. **Patel, S.; Bhirde, A. A.; Rusling, J. F.; Chen, X.; Gutkind, J. S.; Patel, V. Nano delivers big: designing molecular missiles for cancer therapeutics. *Pharmaceutics* 2011, *3* (1), 34-52.**

8. **Spizzirri, U. G.; Curcio, M.; Cirillo, G.; Spataro, T.; Vittorio, O.; Picci, N.; Hampel, S.; Iemma, F.; Nicoletta, F. P. Recent Advances in the Synthesis and Biomedical Applications of Nanocomposite Hydrogels. *Pharmaceutics* 2015, *7* (4), 413-437.**

9. **Zhang, N.; Wardwell, P. R.; Bader, R. A. Polysaccharide-based micelles for drug delivery. *Pharmaceutics* 2013, *5* (2), 329-352.**

10. **Farid, M. M.; Hathout, R. M.; Fawzy, M.; bou-Aisha, K. Silencing of the scavenger receptor (Class B - Type 1) gene using siRNA-loaded chitosan nanaoparticles in a HepG2 cell model. *Colloids Surf. B Biointerfaces* 2014, *123*, 930-937.**

11. **Mehanny, M.; Hathout, R. M.; Geneidi, A. S.; Mansour, S. Exploring the use of nanocarrier systems to deliver the magical molecule; Curcumin and its derivatives. *J Control Release* 2016, *225*, 1-30.**

12. **Mehanny, M.; Hathout, R. M.; Geneidi, A. S.; Mansour, S. Studying the effect of physically-adsorbed coating polymers on the cytotoxic activity of optimized bisdemethoxycurcumin loaded-PLGA nanoparticles. *J Biomed. Mater. Res. A* 2017, *105* (5), 1433-1445.**

13. **Soltani, S.; Sardari, S.; Soror, S. A. Computer simulation of a novel pharmaceutical silicon nanocarrier. *Nanotechnol. Sci Appl.* 2010, *3*, 149-157.**

14. **Fagir, W.; Hathout, R. M.; Sammour, O. A.; ElShafeey, A. H. Self-microemulsifying systems of Finasteride with enhanced oral bioavailability: multivariate statistical evaluation, characterization, spray-drying and in vivo studies in human volunteers. *Nanomedicine (Lond)* 2015, *10* (22), 3373-3389.**

15. **Hathout, R. M.; Metwally, A. A. Towards better modelling of drug-loading in solid lipid nanoparticles: Molecular dynamics, docking experiments and Gaussian Processes machine learning. *Eur. J Pharm Biopharm.* 2016, *108*, 262-268.**

16. **Metwally, A. A.; Hathout, R. M. Computer-Assisted Drug Formulation Design: Novel Approach in Drug Delivery. *Mol Pharm* 2015, *12* (8), 2800-2810.**

17. **Metwally, A. A.; El-Ahmady, S. H.; Hathout, R. M. Selecting optimum protein nano-carriers for natural polyphenols using chemoinformatics tools. *Phytomedicine.* 2016, *23* (14), 1764-1770.**

18. **Metwally, A. A.; Hathout, R. M. Replacing microemulsion formulations experimental solubility studies with in-silico methods comprising molecular dynamics and docking experiments. *Chemical Engineering Research and Design* 2015, *104*, 453-456.**

19. **Hathout, R. M.; El-Ahmady, S. H.; Metwally, A. A. Curcumin or bisdemethoxycurcumin for nose-to-brain treatment of Alzheimer disease? A bio/chemo-informatics case study. *Nat. Prod. Res.* 2017, 1-10.**

20. **Gad, H. A.; El-Ahmady, S. H.; bou-Shoer, M. I.; Al-Azizi, M. M. Application of chemometrics in authentication of herbal medicines: a review. *Phytochem. Anal.* 2013, *24* (1), 1-24.**

21. **Ronowicz, J.; Thommes, M.; Kleinebudde, P.; Krysinski, J. A data mining approach to optimize pellets manufacturing process based on a decision tree algorithm. *Eur. J Pharm Sci* 2015, *73*, 44-48.**

22. **Hathout, R. M. Using principal component analysis in studying the transdermal delivery of a lipophilic drug from soft nano-colloidal carriers to develop a quantitative composition effect permeability relationship. *Pharm Dev. Technol.* 2014, *19* (5), 598-604.**

23. **Singh, S. K.; Verma, P. R.; Razdan, B. Development and characterization of a lovastatin-loaded self-microemulsifying drug delivery system. *Pharm Dev. Technol.* 2010, *15* (5), 469-483.**

24. **Singh, S. K.; Verma, P. R.; Razdan, B. Glibenclamide-loaded self-nanoemulsifying drug delivery system: development and characterization. *Drug Dev. Ind. Pharm* 2010, *36* (8), 933-945.**

25. **Martins, S.; Tho, I.; Souto, E.; Ferreira, D.; Brandl, M. Multivariate design for the evaluation of lipid and surfactant composition effect for optimisation of lipid nanoparticles. *Eur. J Pharm Sci* 2012, *45* (5), 613-623.**

26. **Malzert-Freon, A.; Hennequin, D.; Rault, S. Partial least squares analysis and mixture design for the study of the influence of composition variables on lipidic nanoparticle characteristics. *J Pharm Sci* 2010, *99* (11), 4603-4615.**

27. **Ossama, M.; Hathout, R. M.; Attia, D. A.; Mortada, N. D. Enhanced Allicin Cytotoxicity on HEPG-2 Cells Using Glycyrrhetinic Acid Surface-Decorated Gelatin Nanoparticles. *ACS Omega* 2019, *4* (6), 11293-11300.**

28. **Elzoghby, A. O.; Samy, W. M.; Elgindy, N. A. Protein-based nanocarriers as promising drug and gene delivery systems. *J Control Release* 2012, *161* (1), 38-49.**

29. **Elzoghby, A. O. Gelatin-based nanoparticles as drug and gene delivery systems: reviewing three decades of research. *J Control Release* 2013, *172* (3), 1075-1091.**

30. **Abozeid, S. M.; Hathout, R. M.; bou-Aisha, K. Silencing of the metastasis-linked gene, AEG-1, using siRNA-loaded cholamine surface-modified gelatin nanoparticles in the breast carcinoma cell line MCF-7. *Colloids Surf. B Biointerfaces* 2016, *145*, 607-616.**

31. **Hathout, R. M.; Omran, M. K. Gelatin-based particulate systems in ocular drug delivery. *Pharm Dev. Technol.* 2016, *21* (3), 379-386.**

32. **Jones, R. J.; Rajabi-Siahboomi, A.; Levina, M.; Perrie, Y.; Mohammed, A. R. The influence of formulation and manufacturing process parameters on the characteristics of lyophilized orally disintegrating tablets. *Pharmaceutics* 2011, *3* (3), 440-457.**

33. **Kanth, V. R.; Kajjari, P. B.; Madalageri, P. M.; Ravindra, S.; Manjeshwar, L. S.; Aminabhavi, T. M. Blend Hydrogel Microspheres of Carboxymethyl Chitosan and Gelatin for the Controlled Release of 5-Fluorouracil. *Pharmaceutics* 2017, *9* (2).**

34. **Panizzon, G. P.; Bueno, F. G.; Ueda-Nakamura, T.; Nakamura, C. V.; as Filho, B. P. Preparation of Spray-Dried Soy Isoflavone-Loaded Gelatin Microspheres for Enhancement of Dissolution: Formulation, Characterization and in Vitro Evaluation. *Pharmaceutics* 2014, *6* (4), 599-615.**

35. **Taguchi, K.; Yamasaki, K.; Seo, H.; Otagiri, M. Potential Use of Biological Proteins for Liver Failure Therapy. *Pharmaceutics* 2015, *7* (3), 255-274.**

36. **Xuan, X. Y.; Cheng, Y. L.; Acosta, E. Lecithin-linker microemulsion gelatin gels for extended drug delivery. *Pharmaceutics* 2012, *4* (1), 104-129.**

37. **Kharia, A. A.; Singhai, A. K.; Verma, R. Formulation and evaluation of polymeric nanoparticles of an antiviral drug for gastroretention. *Int. J. Pharm. Sci. Nanotechnol.* 2012, *4* (4), 1557-1562.**

38. **Khatik, R.; Dwivedi, P.; Khare, P.; Kansal, S.; Dube, A.; Mishra, P. R.; Dwivedi, A. K. Development of targeted 1,2-diacyl-sn-glycero-3-phospho-l-serine-coated gelatin nanoparticles loaded with amphotericin B for improved in vitro and in vivo effect in leishmaniasis. *Expert Opin. Drug Deliv.* 2014, *11* (5), 633-646.**

39. **Kuntworbe, N.; Al-Kassas, R. Design and in vitro haemolytic evaluation of cryptolepine hydrochloride-loaded gelatine nanoparticles as a novel approach for the treatment of malaria. *AAPS PharmSciTech* 2012, *13* (2), 568-581.**

40. **Leo, E.; ngela Vandelli, M.; Cameroni, R.; Forni, F. Doxorubicin-loaded gelatin nanoparticles stabilized by glutaraldehyde: Involvement of the drug in the cross-linking process. *International Journal of Pharmaceutics* 1997, *155* (1), 75-82.**

41. **Naidu, B. V. K.; Paulson, A. T. A new method for the preparation of gelatin nanoparticles: Encapsulation and drug release characteristics. *J. Appl. Polym. Sci.* 2011, *121* (6), 3495-3500.**

42. **Saraogi, G. K.; Sharma, B.; Joshi, B.; Gupta, P.; Gupta, U. D.; Jain, N. K.; Agrawal, G. P. Mannosylated gelatin nanoparticles bearing isoniazid for effective management of tuberculosis. *J Drug Target* 2011, *19* (3), 219-227.**

43. **Karthikeyan, S.; Rajendra Prasad, N.; Ganamani, A.; Balamurugan, E. Anticancer activity of resveratrol-loaded gelatin nanoparticles on NCI-H460 non-small cell lung cancer cells. *Biomedicine & Preventive Nutrition* 2013, *3* (1), 64-73.**

44. **Metwally, A. A.; El-Ahmady, S. H.; Hathout, R. M. Selecting optimum protein nano-carriers for natural polyphenols using chemoinformatics tools. *Phytomedicine.* 2016, *23* (14), 1764-1770.**

45. **Lu, Z.; Yeh, T. K.; Wang, J.; Chen, L.; Lyness, G.; Xin, Y.; Wientjes, M. G.; Bergdall, V.; Couto, G.; varez-Berger, F.; Kosarek, C. E.; Au, J. L. Paclitaxel gelatin nanoparticles for intravesical bladder cancer therapy. *J Urol.* 2011, *185* (4), 1478-1483.**

46. **Kumar, R.; Nagarwal, R. C.; Dhanawat, M.; Pandit, J. K. In-vitro and in-vivo study of indomethacin loaded gelatin nanoparticles. *J Biomed. Nanotechnol.* 2011, *7* (3), 325-333.**

47. **Kumar, R.; Nagarwal, R. C.; Dhanawat, M.; Pandit, J. K. In-vitro and in-vivo study of indomethacin loaded gelatin nanoparticles. *J Biomed. Nanotechnol.* 2011, *7* (3), 325-333.**

48. **Spjuth, O.; Helmus, T.; Willighagen, E. L.; Kuhn, S.; Eklund, M.; Wagener, J.; Murray-Rust, P.; Steinbeck, C.; Wikberg, J. E. Bioclipse: an open source workbench for chemo- and bioinformatics. *BMC Bioinformatics* 2007, *8*, 59.**

49. **Milligan, G. W. An examination of the effect of six types of error perturbation on fifteen clustering algorithms. *Psychometrika* 1980, *45* (3), 325-342.**

50. **Pronk, S.; Pall, S.; Schulz, R.; Larsson, P.; Bjelkmar, P.; Apostolov, R.; Shirts, M. R.; Smith, J. C.; Kasson, P. M.; van der, S. D.; Hess, B.; Lindahl, E. GROMACS 4.5: a high-throughput and highly parallel open source molecular simulation toolkit. *Bioinformatics* 2013, *29* (7), 845-854.**

51. **Vanommeslaeghe, K.; Hatcher, E.; Acharya, C.; Kundu, S.; Zhong, S.; Shim, J.; Darian, E.; Guvench, O.; Lopes, P.; Vorobyov, I.; Mackerell, A. D., Jr. CHARMM general force field: A force field for drug-like molecules compatible with the CHARMM all-atom additive biological force fields. *J Comput Chem.* 2010, *31* (4), 671-690.**

52. **Abdel-Hafez, S. M.; Hathout, R. M.; Sammour, O. A. Tracking the transdermal penetration pathways of optimized curcumin-loaded chitosan nanoparticles via confocal laser scanning microscopy. *Int. J Biol Macromol.* 2018, *108*, 753-764.**

53. Spjuth, O.; Helmus, T.; Willighagen, E. L.; Kuhn, S.; Eklund, M.; Wagener, J.; Murray-Rust, P.; Steinbeck, C.; Wikberg, J. E. Bioclipse: an open source workbench for chemo- and bioinformatics. *BMC Bioinformatics* 2007, *8*, 59.

54. Hathout, R. M.; El-Ahmady, S. H.; Metwally, A. A. Curcumin or bisdemethoxycurcumin for nose-to-brain treatment of Alzheimer disease? A bio/chemo-informatics case study. *Nat. Prod. Res.* 2018, *32* (24), 2873-2881.

55. Gad, H. A.; El-Ahmady, S. H.; bou-Shoer, M. I.; Al-Azizi, M. M. Application of Chemometrics in Authentication of Herbal Medicines: A Review. *Phytochem. Anal.* 2012.

56. Hathout, R. M.; Metwally, A. A. Gelatin Nanoparticles. *Methods Mol Biol* 2019, *2000*, 71-78.

57. Hellberg, S.; Sjostrom, M.; Skagerberg, B.; Wold, S. Peptide quantitative structure-activity relationships, a multivariate approach. *J Med. Chem.* 1987, *30* (7), 1126-1135.

58. Junaid, M.; Lapins, M.; Eklund, M.; Spjuth, O.; Wikberg, J. E. Proteochemometric modeling of the susceptibility of mutated variants of the HIV-1 virus to reverse transcriptase inhibitors. *PLoS One* 2010, *5* (12), e14353.

59. Lapins, M.; Wikberg, J. E. Kinome-wide interaction modelling using alignment-based and alignment-independent approaches for kinase description and linear and non-linear data analysis techniques. *BMC Bioinformatics* 2010, *11*, 339.

60. Strombergsson, H.; Lapins, M.; Kleywegt, G. J.; Wikberg, J. E. Towards Proteome-Wide Interaction Models Using the Proteochemometrics Approach. *Mol Inform.* 2010, *29* (6-7), 499-508.

61. Sandberg, M.; Eriksson, L.; Jonsson, J.; Sjostrom, M.; Wold, S. New chemical descriptors relevant for the design of biologically active peptides. A multivariate characterization of 87 amino acids. *J Med. Chem.* 1998, *41* (14), 2481-2491.

62. Maccari, G.; Di, L. M.; Nifosi, R.; Cardarelli, F.; Signore, G.; Boccardi, C.; Bifone, A. Antimicrobial peptides design by evolutionary multiobjective optimization. *PLoS Comput Biol* 2013, *9* (9), e1003212.

63. Wold, S.; Jonsson, J.; Sj+Ârstr+Âm, M.; Sandberg, M.; R+ñnnar, S. DNA and peptide sequences and chemical processes multivariately modelled by principal component analysis and partial least-squares projections to latent structures. *Analytica Chimica Acta* 1993, *277* (2), 239-253.

64. Wang, R.; Lai, L.; Wang, S. Further development and validation of empirical scoring functions for structure-based binding affinity prediction. *J Comput Aided Mol Des* 2002, *16* (1), 11-26.